Journal of Organometallic Chemistry 694 (2009) 1549–1556

Contents lists available at ScienceDirect

Journal of Organometallic Chemistry

journal homepage: www.elsevier.com/locate/jorganchem

Combined experimental and computational study of W(II), Ru(II), Pt(IV) and Cu(I) amine and amido complexes using ^{15}N NMR spectroscopy

Samuel A. Delp [a], Colleen Munro-Leighton [a], Chetna Khosla [b], Joseph L. Templeton [b], Nikki M. Alsop [a], T. Brent Gunnoe [a,*], Thomas R. Cundari [c,*]

[a] Department of Chemistry, University of Virginia, Charlottesville, VA 22904, United States
[b] W.R. Kenan Laboratory, Department of Chemistry, University of North Carolina, Chapel Hill, NC 27599-3290, United States
[c] Center for Advanced Scientific Computing and Modeling (CASCaM), Department of Chemistry, University of North Texas, Box 305070, Denton, TX 76203-5070, United States

ARTICLE INFO

Article history:
Received 3 December 2008
Received in revised form 7 January 2009
Accepted 8 January 2009
Available online 14 January 2009

Keywords:
^{15}N NMR spectroscopy
Transition metals
Amido
Amine

ABSTRACT

Using 2D proton-coupled gHSQC pulse sequences in addition to 1D ^{15}N NMR experiments of ^{15}N labeled systems, ^{15}N NMR chemical shifts of a range of transition metal amido and amine complexes were determined. Tungsten(II), ruthenium(II), platinum(IV) and copper(I) complexes with aniline and their anilido variants were studied and compared to free aniline, lithium anilido and anilinium tetrafluoroborate. Upon coordination of aniline to transition metals, upfield chemical shifts of 20–60 ppm were observed. Deprotonation of the amine complexes to form amido complexes resulted in downfield chemical shifts of 40–60 ppm for all of the complexes except for the tungsten d^4 system. For the tungsten(II) complexes, the cationic aniline complex displayed a downfield shift of approximately 56 ppm relative to the neutral anilido complex. The change in chemical shift for amine to amido conversion is proposed to depend on the ability of the amido ligand to π-bond with the metal center, which influences the magnitude of the paramagnetic screening term.

1. Introduction

Anionic heteroatomic ligands (*e.g.* amido, oxo, imido, alkoxo, hydroxo, thiolate) exhibit diverse properties that depend on metal identity and the formal oxidation state of the metal. For example, amido (NR_2^-) and imido (NR^{2-}) moieties have been utilized as inert ancillary ligands as well as reactive ligands central to metal-mediated catalysis [1–13]. When coordinated to transition metals with one or more vacant dπ orbital(s), amido ligands can function as strong π-donors to produce metal-amido multiple bonding (Scheme 1) [14–26]. The amido-to-metal π-interaction reduces the electron density at the amido ligand and, hence, can decrease, in some cases substantially, the propensity of this ligand to react as a basic or nucleophilic center [18,19]. In contrast, coordination to metal centers with a filled dπ manifold formally disrupts amido-to-metal π-bonding since both π and π* molecular orbitals are filled (Scheme 1) [27,28]. This bonding scenario can enhance ligand-centered reactivity by increasing the basicity and/or nucleophilicity of the heteroatomic ligand relative to systems in which amido-to-metal π-bonding is present [2–4,27–37].

Examples of amido complexes in which metal-amido π-bonding is disrupted are predominantly found for the late transition metals. For example, Bergman *et al.* have reported a Ru(II) parent amido complex that is capable of deprotonating the C–H bond of weak acids such as phenylacetylene, fluorene and triphenylmethane [29,38]. Ruthenium in the plus two oxidation state, as in, $TpRuL_2(NHR)$, $TpRu(PMe_3)_2OR$ and (PCP)Ru(CO)NHR {Tp = hydridotris(pyrazolyl)borate; L = PMe_3 or $P(OMe)_3$; PCP = 2,6-$(CH_2P^tBu_2)_2C_6H_3$} complexes, undergoes reactions indicative of nucleophilic amido and alkoxo/hydroxo ligands [30,32,33,39–43]. Single electron oxidation to Ru(III) increases the predilection toward odd electron radical reactions [40]. An octahedral Fe(II) parent amido complex possesses sufficient nucleophilicity at nitrogen to undergo an apparent intermolecular nucleophilic addition to *free* carbon monoxide [44,45].

Recognition of the importance of ligand-to-metal π-donation for tuning the reactivity of formally anionic (or dianionic) heteroatomic ligands has sparked efforts to understand the relationship between M–X (X = NR_2, OR, O, NR, *etc.*) bonding and the reactivity of such complexes [2–5,18,27,28,32,33,37,38,40,42,45–59]. Along these lines, our groups have been pursuing the synthesis and reactivity of transition metal complexes with non-dative heteroatomic ligands. Collectively, we have studied the reactivity of W(II), Ru(II), Pt(IV), and Cu(I) systems with amido, alkoxo and related ligands [2,15,16,30–37,41,43,60–63]. The Ru(II), Pt(IV) and Cu(I) systems all exhibit reactivity that can be attributed, at least in part, to the disruption of ligand-to-metal π-donation.

Despite the increased attention recently focused on late transition metals in low oxidation states with amido ligands, to our

* Corresponding authors.
E-mail addresses: tbg7h@virginia.edu (T.B. Gunnoe), t@unt.edu (T.R. Cundari).

0022-328X/$ - see front matter © 2009 Elsevier B.V. All rights reserved.
doi:10.1016/j.jorganchem.2009.01.006

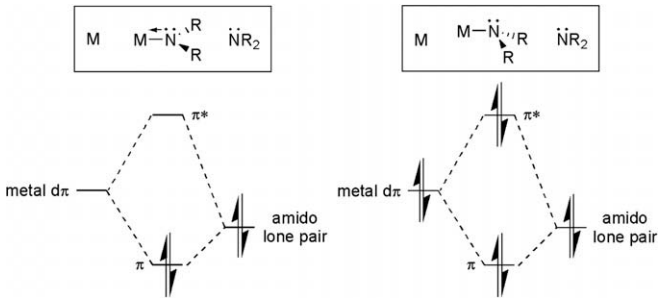

Scheme 1. Stabilization of amido lone pair via π-donation into an empty d-orbital versus interaction with filled dπ orbital. On the left, the filled metal-nitrogen π molecular orbital results in multiple bonding, while filled π and π* molecular orbitals (on the right) result in no net M–N multiple bonding.

knowledge a systematic study of such systems using ^{15}N NMR spectroscopy has not been reported. In fact, despite increased use of ^{15}N NMR spectroscopy in the study of solid-state and biological systems [64–72], the application of ^{15}N NMR spectroscopy to solution phase transition metal chemistry is relatively rare [73–75]. The dearth of ^{15}N NMR data for metal amido (and related) complexes is due in large part to the low natural abundance and low sensitivity of the ^{15}N nucleus [73]. Given the large chemical shift range of ^{15}N nuclei, ^{15}N NMR spectroscopy potentially can provide a wealth of information about structure, bonding and reactivity of amido and related transition metal systems. However, in order to exploit this tool, a database of ^{15}N NMR data and chemical shift trends tabulating metal oxidation state, electron configuration and electron count must be established.

Herein, we report on ^{15}N NMR spectroscopy of Ru(II), Pt(IV), and Cu(I) amido complexes and the corresponding amine systems. The chemical shifts of these systems are compared to the benchmarks set by the aniline, [Li][NHPh], and $[NH_3Ph]^+$ triad; data for a pair of amido and amine W(II) complexes, Tp*W(CO)(PhC≡CMe)(NHPh) and $[Tp^*W(CO)(PhC{\equiv}CMe)(NH_2Ph)][BAr'_4]$ {Tp* = hydridotris(3,5-dimethylpyrazolyl)borate; Ar' = 3,5-$(CF_3)_2C_6H_3$}, are also included. In addition to initiating a database of ^{15}N NMR data, these studies were designed to probe the potential impact of the presence/absence of amido-to-metal π-bonding on chemical shifts (Scheme 1). Computational studies have been used in combination with the experimental data in an effort to model and understand the ^{15}N NMR data.

2. Results and discussion

2.1. Experimental results

For this study, we selected a range of systems for which amido-to-metal π-bonding is blocked by filled dπ manifolds (Chart 1). The Ru(II) and Pt(IV) complexes are d^6 and six-coordinate and, hence, are electronically saturated 18-electron species in the absence of amido-to-metal π-donation. For these complexes, there are no vacant metal-based orbitals of π-symmetry. We have previously shown that the Ru(II) systems exhibit basic and nucleophilic character at the amido ligand, which is likely due to the disruption of amido-to-ruthenium π-donation [30,33,43,62]. The two-coordinate Cu(I) system is formally a 14-electron species in the absence of amido π-donation, and previously reported studies indicate insignificant amido-Cu π-interaction [37]. Indeed, for (IPr)-Cu(NHPh), joint experimental/computational studies suggest more significant π-bonding between the amido N and ipso C of the phenyl substituent than between the amido N and Cu [31,37]. For the Ru(II), Pt(IV) and Cu(I) systems, we also acquired ^{15}N NMR data for the cationic amine complexes to determine the impact of protonation on the ^{15}N NMR chemical shifts.

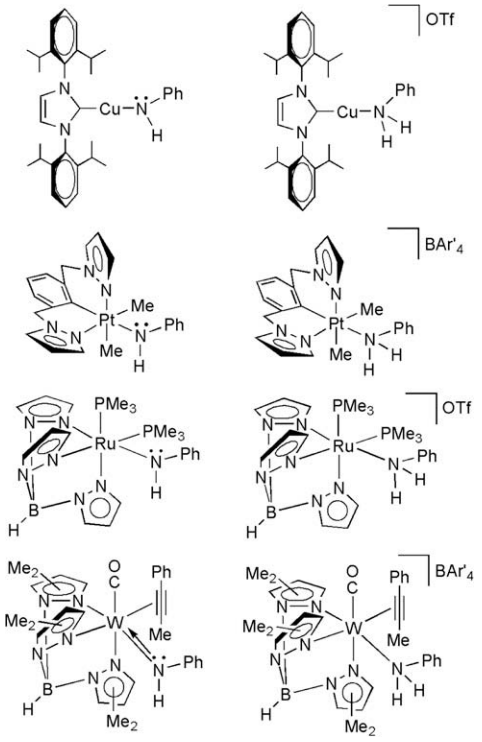

Chart 1. Transition metal amido and amine complexes studied herein.

As a contrast to the Ru, Pt and Cu systems for which amido-metal π-interaction is expected to be minimal, we obtained ^{15}N NMR spectra of an amido/amine pair that is coordinated to a metal with a vacant dπ orbital. The previously reported six-coordinate W(II) (d^4) complex Tp*W(CO)(PhC≡CMe)NHPh possesses an empty dπ orbital and engages in W-amido multiple bonding, albeit in competition with alkyne $\pi_\perp$ to W π-donation [16]. Previous studies are consistent with W-N_{amido} multiple bonding as evidenced by spectroscopic data of the complexes $[Tp^*W(CO)(PhC{\equiv}CMe)NH_nPh]^{m+}$ ($n = 1$, $m = 0$; $n = 2$, $m = 1$) [16]. For example, the ^{13}C NMR spectrum of Tp*W(CO)(PhC≡CMe)NHPh reveals chemical shifts at 178.3 and 181.3 ppm for the alkyne carbons, consistent with π-donation from both the alkyne and amido ligands into a single vacant dπ orbital. In contrast, the cationic amine complex, $[Tp^*W(CO)(PhC{\equiv}CMe)NH_2Ph]^+$, exhibits alkyne resonances at 214.9 and 216.4 ppm, which reflect a four-electron donor alkyne [73–75].

2.2. ^{15}N NMR spectroscopy

NMR spectroscopy is routinely used to characterize organic compounds and organometallic complexes with ^{1}H, ^{13}C, ^{19}F and ^{31}P NMR the most commonly studied nuclei. These isotopes offer either high or reasonable natural abundance as well as good NMR sensitivity, which combine to allow rapid acquisition of high quality spectra. The ^{15}N ($I = ½$) isotope is an NMR active nucleus present in many organic and organometallic compounds; however, ^{15}N NMR spectroscopy data acquisition is not yet routine due to the low natural abundance of the ^{15}N isotope (0.37%) and poor signal intensity [74,76]. Isotopic labeling can facilitate the acquisition of ^{15}N NMR spectroscopy data, but label incorporation is expensive and can be time consuming. With advancements in 2D NMR analysis and methods such as gHMBC (gradient heteronuclear multiple bond coherence) and gHSQC (gradient heteronuclear single quantum coherence), techniques for obtaining ^{15}N chemical shifts from compounds in the absence of isotopic enrichment have become more accessible. For the complexes shown in Chart 1, we acquired

^{15}N NMR data using proton-coupled gHSQC experiments. This 2D method of ^{15}N NMR only detects N atoms that have protons directly bonded, which is advantageous herein since pyrazolyl and imidazolyl N atoms remain "silent" and only the amido or amine N atoms of the transition metal complexes are detected. In some cases, obtaining reliable signal-to-noise ratio was difficult using the 2D methods, and in these cases the ^{15}N NMR data were acquired using the ^{15}N labeled complexes and standard 1D ^{15}N NMR experiments. The ^{15}N NMR spectra were referenced to aniline, which was set to 0 ppm.

Table 1 displays the ^{15}N chemical shifts that were acquired in THF-d_8. To establish a baseline for change in chemical shift upon converting from amine to amido, we first obtained ^{15}N NMR spectra of aniline and the anilido salt Li[NHPh]. The deprotonated species Li[NHPh] has a downfield chemical shift of 44.4 ppm compared to the resonance for aniline. Our observation of a downfield chemical shift of approximately 44 ppm upon converting aniline to its lithium anilido salt is consistent with previously reported ^{15} NMR data. For example, Ide *et al.* have reported downfield chemical shifts (in THF) of lithium anilides relative to anilines between 35.7 and 42.4 ppm [77,78]. For all complexes studied, the coordination of aniline to transition metals results in upfield chemical shifts. For example, the ruthenium(II) aniline complex [TpRu(P-Me$_3$)$_2$(NH$_2$Ph)][OTf] has a ^{15}N NMR resonance at −62.1 ppm. In comparison, the protonation of aniline to form the anilinium species [NH$_3$Ph][BF$_4$] results in a minor upfield shift to approximately −6 ppm [78]. Thus, coordination of NH$_2$Ph to ruthenium(II) {or to W(II) or Pt(IV), see below} has a much greater impact on chemical shift than protonation (Chart 2). The ruthenium(II) anilido complex TpRu(PMe$_3$)$_2$(NHPh) exhibits a resonance at −3.1 ppm (Fig. 1), which is upfield compared to lithium anilido salt at 44.4 ppm. The conversion of [TpRu(PMe$_3$)$_2$(NH$_2$Ph)]$^+$ to TpRu(PMe$_3$)$_2$NHPh results in a downfield chemical shift of approximately 59 ppm.

The coordination of aniline to the platinum cation [(NCN)Pt-(Me)$_2$]$^+$ {NCN = 2,6-(pyrazolyl-CH$_2$)$_2$C$_6$H$_3$} gives results similar to coordination to Ru(II) with a ^{15}N chemical shift of −23.5 ppm (upfield of free aniline) for the platinum complex. The platinum anilido species, (NCN)Pt(Me)$_2$NHPh, has a resonance at 15.9 ppm with $^1J_{PtN}$ = 209 Hz (Fig. 2), which is shifted upfield compared to the lithium anilido species. Thus, similar to the [TpRu(PMe$_3$)$_2$(NH$_n$Ph)]^m (n = 1, m = 0; n = 2, m = +1) system, the conversion of the Pt-aniline complex to Pt-anilido results in a downfield chemical shift with $\Delta\delta$ = 39.4 ppm. The difference in magnitude of the aniline/anilido chemical shifts for Pt(IV) is less than Ru(II) with the latter exhibiting a $\Delta\delta$ of 59.0 ppm.

The aniline complex [Tp*W(CO)(η^2-PhC≡CMe)(NH$_2$Ph)][BAr'$_4$] was found to have a ^{15}N NMR resonance at −19.5 ppm. The tungsten anilido complex, Tp*W(CO)(η^2-PhC≡CMe)(NHPh), displays an N^{15} shift of −75.1 ppm, which is more than 55 ppm *upfield* compared to the aniline complex. In contrast, comparison of aniline

Table 1
^{15}N NMR chemical shifts (ppm) acquired using proton-coupled gHSQC experiments or standard 1D ^{15}N NMR with isotopically enriched samples {aniline was used as an external reference at 0 ppm and all data were acquired in THF-d_8; Tp = hydridotris(pyrazolyl)borate; Tp* = hydridotris(3,5-dimethylpyrazolyl)borate; IPr = 1,3-bis(2,6-diisopropylphenyl)imidazol-2-ylidene}.

Compound	δ[a]	$\Delta\delta$[b]
[Li][NHPh]	44.4[c]	44.4
NH$_2$Ph	0.0[c,d]	6[f]
[NH$_3$Ph][BF$_4$]	−6[e]	
TpRu(PMe$_3$)$_2$(NHPh)	−3.1[c]	59.0
[TpRu(PMe$_3$)$_2$(NH$_2$Ph)][OTf]	−62.1[c]	
(NCN)Pt(Me)$_2$(NHPh)	15.9[d,g]	39.4
[(NCN)Pt(Me)$_2$(NH$_2$Ph)][BAr'$_4$]	−23.5[c]	–
Tp*W(CO)(η^2-PhC≡CMe)(NHPh)	−75.3[d,h]	−55.8
[Tp*W(CO)(η^2-PhC≡CMe)(NH$_2$Ph)][BAr'$_4$]	−19.5[d]	
(IPr)Cu(NHPh)	30.9[c]	N/A
[(IPr)Cu(NH$_2$Ph)][OTf]	N/A	

[a] Chemical shift (ppm).
[b] $\delta_{amido} - \delta_{amine}$.
[c] Acquired via 2D gHSQC experiment.
[d] Acquired via standard 1D ^{15}N NMR experiment with isotopically enriched sample.
[e] Data from Ref. [78].
[f] $\delta_{aniline} - \delta_{anilinium}$.
[g] $^1J_{Pt-N}$ = 209 Hz.
[h] $^1J_{W-N}$ = 61 Hz.

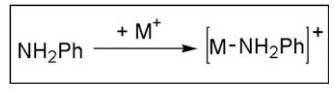

M	Δδ
H	6.0
TpRu(PMe$_3$)$_2$	62.1
(NCN)Pt(Me)$_2$	23.5
Tp*W(CO)(PhC$_2$Me)	19.5

Chart 2. Comparison of impact on chemical shift of protonation of aniline versus coordination to various transition metal cations ($\Delta\delta = \delta_{aniline} - \delta_{M-NH_2Ph}$).

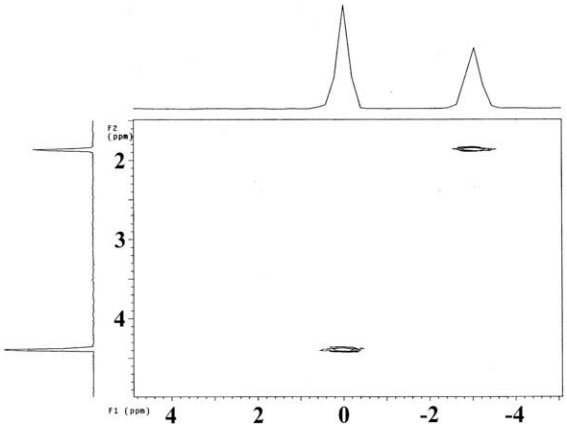

Fig. 1. 2D gHSQC NMR spectra overlay of aniline and TpRu(PMe$_3$)$_2$NHPh. The ^{15}N NMR spectrum is located on the *x*-axis with the peak at 0.00 ppm due to aniline and the peak at −3.1 ppm due to TpRu(PMe$_3$)$_2$NHPh. The ^{1}H NMR spectrum is on the *y*-axis.

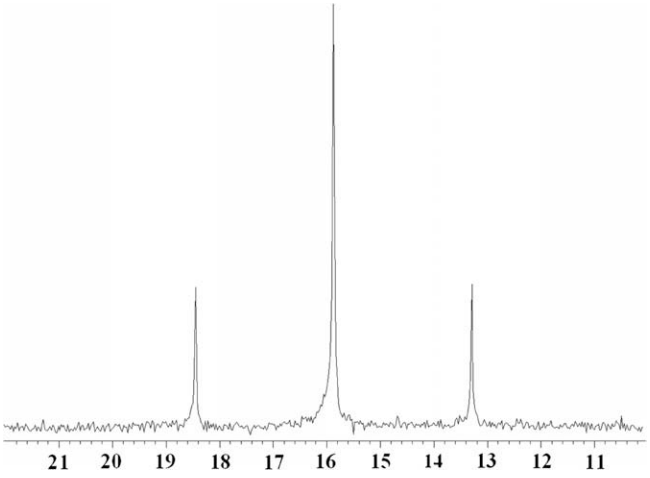

Fig. 2. ^{15}N NMR spectrum of (NCN)Pt(Me)$_2$*NHPh that displays satellites due to ^{195}Pt–*N coupling (*N = ^{15}N).

and anilido complexes reveals downfield chemical shifts for the Ru(II) and Pt(IV) systems. The tungsten–amido complex is the only complex whose formal d electron configuration allows amido-to-metal multiple bonding. The presence of multiple bonding may account for the difference in chemical shift upon converting from aniline to anilido complexes for Ru(II) and Pt(IV) versus W(II) (see below). For the tungsten amido complex Tp*W(CO)-(η^2-PhC≡CMe)(NHPh), satellites due to ^{183}W–^{15}N coupling ($^1J_{WN}$ = 61 Hz) were observed.

The copper amido complex (IPr)Cu(NHPh) has a ^{15}N NMR chemical shift of 30.9 ppm, which is the most substantial downfield shift observed of all of the transition metal complexes in this study. Unfortunately, we were unable to obtain an experimental chemical shift for the copper–amine complex from 2D or 1D ^{15}N NMR experiments performed in various different solvents. The theoretical chemical shift of the copper-amine complex will be described below.

2.3. Computational studies

Calculated ^{15}N NMR chemical shifts in the gas-phase and THF solvent are given in Table 2. Comparison of calculated ^{15}N chemical shifts in gas-phase and in THF show similar agreement in relation to experimental numbers, and thus our analysis will focus on the latter as it is more appropriate to the experimental conditions. In both solution and gas-phase, the calculated chemical shift of the W–anilido complex Tp*W(CO)(η^2-PhC≡CMe)(NHPh) is an obvious outlier. A plot of the calculated (THF) versus experimental ^{15}N NMR chemical shifts is shown in Fig. 3. When the single outlier for Tp*W(CO)(η^2-PhC≡CMe)(NHPh) is removed, agreement between experimental and calculated data is good (R^2 = 0.92).

In general, agreement between calculated and experimental ^{15}N NMR chemical shifts is good with the exception of Tp*W(CO)(η^2-PhC≡CMe)(NHPh). It is possible that the d^4 electron configuration gives rise to accessible electronic transitions and a larger paramagnetic contribution for the W–anilido complex (see below). Tp*W(CO)(η^2-PhC≡CMe)(NHPh) is the only complex studied that possesses a vacant metal d orbital, which enables amido-to-metal π-bonding. The calculated W–N bond length is short at 2.02 Å (in comparison to the sum of the W and N covalent radii), and the various angular metrics about the anilido N suggest that it is close to planar (sum of angles at N = 359.5° and the W–N–H···C_{ipso} improper torsion angle = 174°), supporting the inference of multiple bond character in the W–N bond. Appropriate caution must be exercised, however, in using amido planarity to indicate the presence or absence of π-bonding with a metal center [79]. In a previous study of Cu–anilido complexes by our groups, the anilido N was also found to be planar [37], but in that case amido planarity was ascribed to N–C_{ipso} π-bonding rather than metal-amido multiple bonding. The experimentally determined short N–C_{ipso} bond lengths for a series of Cu(I) anilido complexes of ~1.35 Å, which are shorter than typical N–C single bonds (~1.47 Å), are consistent with a substantial degree of N–C_{ipso} multiple bonding. The corresponding bond distance of the amine complex [(dtbpe)-Cu(NH_2Ph)][PF_6] is longer at 1.444(4) Å. For the W amido complex, the calculated N–C_{ipso} bond length is considerably longer at 1.41 Å, again supporting the hypothesis that there is significant metal-amido multiple bond character in Tp*W(CO)(η^2-PhC≡CMe)(NHPh).

Table 2
DFT-calculated ^{15}N NMR chemical shifts for amido and amine species in gas-phase and in THF solvent.

Compound	Experimental δ[a]	Calculated/ gas δ	Calculated/ THF δ
[Li][NHPh]	44.4	70.1	53.0
NH_2Ph	0.0	0.0	0.0
TpRu(PMe_3)$_2$(NHPh)	−3.1	−4.5	15.5
[TpRu(PMe_3)$_2$(NH_2Ph)][OTf]	−62.1	−30.2	−29.9
(NCN)Pt(Me)$_2$NHPh	15.9	20.5	24.7
[(NCN)Pt(Me)$_2$(NH_2Ph)][BAr′$_4$]	−23.5	−7.3	−5.9
Tp*W(CO)(η^2-PhC≡CMe)(NHPh)	−75.3	151.2	148.7
[Tp*W(CO)(η^2-PhC≡CMe)(NH_2Ph)][BAr′$_4$]	−19.5	−4.5	−2.3
(IPr)Cu(NHPh)	30.9	26.3	24.0
[(IPr)Cu(NH_2Ph)][OTf]	N/A	−21.3	−18.4

[a] See Table 1 for details.

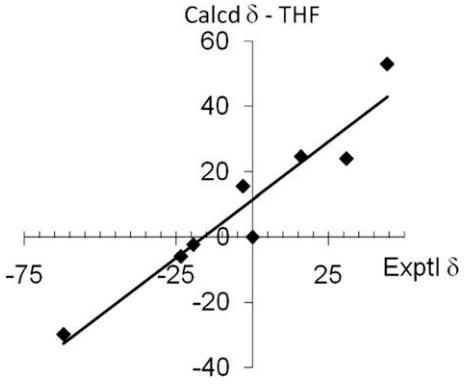

Fig. 3. Plot of calculated (THF) versus experimental ^{15} N NMR chemical shifts (ppm) with the Tp*W(CO)(η2-PhC≡CMe)(NHPh) outlier removed. Axes are in ppm and chemical shifts are referenced to aniline. Least-squares line is y = 0.711 x + 11.39 with an R^2 value of 0.92.

2.4. Discussion

The chemical shift in ^{15}N NMR spectroscopy is determined by the relative contributions of the diamagnetic screening (σ^d) and the paramagnetic screening (σ^p). The paramagnetic term, which often dominates for ^{15}N NMR spectroscopy, has been related to three contributions (Eq. (1)) where ΔE is a function of the energy of accessible electronic transitions, the radial term r^3 is an average of the non-s orbital radius, and Q is a function of bond orders and charge densities of all bonding electrons and is dependent on the extent of multiple bonding [73,74,80].

$$\sigma^p \sim \frac{1}{\Delta E} \cdot \frac{1}{r^3} \cdot \sum Q \qquad (1)$$

In order to delineate possible structural and electronic factors for these amido complexes, a QSPR (quantitative structure property relationship) analysis was performed on the calculated ^{15}N NMR chemical shifts using the MOE (Molecular Operating Environment) package [81]. Descriptors that were evaluated for their impact on the ^{15}N NMR chemical shift (values calculated in THF solvent were used) included the d-electron count of the metal, the calculated Kohn–Sham (KS)-HOMO and KS-LUMO energies, the calculated KS-HOMO/KS-LUMO gap, the calculated anisotropy on the NMR nucleus of interest, the calculated (Mulliken) atomic charge on the amine/amido nitrogen, the number of hydrogen atoms on the amine/amido nitrogen, and whether or not the ligand is an anilido or not (Table 3). Utilizing partial least squares fitting techniques to perform a multiple linear regression yielded a good correlation (Fig. 4; R^2 = 0.99). The best parsimonious QSPR fit (limited to a maximum of 3 descriptors given the small size of the computational dataset) indicated that the most significant of the aforementioned descriptors in determining the calculated ^{15}N chemical shift, as well as the differences between the corresponding amine/amido shifts for the different pairs, is the calculated anisotropy (relative importance = 0.54), the HOMO energy (relative importance = 0.62), and

Table 3
DFT-calculated ^{15}N NMR chemical shifts and QSPR descriptors for amido and amine species in THF solvent [a].

Complex	δ (ppm)	Aniso (ppm)	HOMO (a.u.)	LUMO (a.u.)	Gap (a.u.)	q_N (e$^-$)	q'_N (e$^-$)	d^n (e$^-$)	Anilido
(IPr)Cu(NHPh)	24.0	76.7	−0.2041	0.0169	0.2211	−0.85	−0.49	10	1
[(IPr)Cu(NH$_2$Ph)][OTf]	−18.4	71.4	−0.2883	−0.0042	0.2841	−0.86	0.00	10	1
(NCN)Pt(Me)$_2$(NHPh)	24.7	74.1	−0.2090	0.0301	0.2391	−0.81	−0.46	6	1
[(NCN)Pt(Me)$_2$(NH$_2$ Ph)][BAr'$_4$]	−5.9	64.5	−0.2861	−0.0039	0.2822	−0.82	0.05	6	1
TpRu(PMe$_3$)$_2$(NH$_2$)[b]	−106.3	138.3	−0.2002	0.0407	0.2408	−1.15	−0.49	6	0
[TpRu(PMe$_3$)$_2$(NH$_3$)]$^+$	−79.0	56	−0.2645	0.0184	0.2828	−0.86	0.36	6	0
TpRu(PMe$_3$)$_2$(NHPh)	15.5	114.2	−0.1796	0.0479	0.2275	−0.66	−0.29	6	1
[TpRu(PMe$_3$)$_2$(NH$_2$Ph)][OTf]	−29.9	96.5	−0.2670	0.0188	0.2858	−0.72	0.11	6	1
[{W}(NH$_2$Ph)][BAr'$_4$][c]	−2.3	57.6	−0.2581	−0.0484	0.2097	−0.83	0.04	4	1

[a] The computed descriptors are determined at the same level of theory used to calculate the ^{15}N NMR chemical shifts (see Section 4.3). The quantity δ is the ^{15}N chemical shift (ppm) and Anisotropy (Aniso, ppm) of the nucleus of interest calculated in THF solution, the Kohn–Sham HOMO and LUMO energies (a.u.), the energy difference (gap, a.u.) between the HOMO and LUMO, the Mulliken atomic charge (e$^-$) on the nucleus of interest (q_N), this same quantity with the attached hydrogen charges summed in (q'_N) the formal d orbital occupancy (d^n), and a logical variable (anilido) denoting whether or not ($T = 1$, $F = 0$) the amine/amido has an aromatic substituent.

[b] TpRu(PMe$_3$)$_2$(NH$_x$) data were not discussed Section 4 since the amido complex, TpRu(PMe$_3$)$_2$NH$_2$, is not sufficiently stable in solution to acquire data. The experimental ^{15}N NMR chemical shift of [TpRu(PMe$_3$)$_2$NH$_3$][OTf] is −98.44 ppm.

[c] {W} = Tp*W(CO)(PhC$_2$Me).

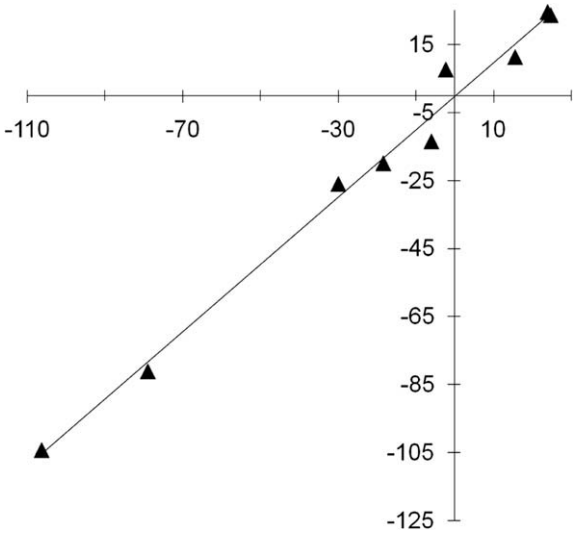

Fig. 4. Plot of QSPR-fit (y-axis) and DFT-calculated (x-axis) ^{15}N NMR chemical shifts for inorganic amido/amines. Least-squares line is given ($R^2 = 0.99$).

whether or not the N nucleus of interest was an anilido (relative importance = 1.00). The HOMO–LUMO gap, the LUMO energy, the calculated atomic charge on the nitrogen, and the formal d electron count were deemed by the QSPR fit to be less significant for determining the ^{15}N shift. Of course, the limitations on calculations of HOMO–LUMO gaps (especially the LUMO energy) must be taken into consideration. The potential impact of the HOMO–LUMO gap (*i.e.* energy of electronic excitation) is discussed in more detail below.

2.5. Impact of d-electron count

A primary motivation for these studies was to compare the influence of amido-metal π-bonding on the ^{15}N NMR chemical shift data. From the experimental data, for the systems in which the d electron count inhibits amido-to-metal π-donation {*i.e.* the Ru(II) and Pt(IV) systems}, the conversion of aniline complexes to amido via proton loss results in a downfield chemical shift. For the Ru(II) complexes, the $\Delta\delta$ ($\delta_{\text{amido complex}} - \delta_{\text{aniline complex}}$) is 59.0 ppm, and the $\Delta\delta$ for the Pt complexes is 39.4 ppm. Although we could not obtain an experimental ^{15}N NMR chemical shift for [(IPr)Cu(NH$_2$Ph)][OTf], the calculated data reflect a similar trend to the Ru(II) and Pt(IV) complexes. Upon conversion of Cu amine [(IPr)Cu(NH$_2$Ph)][OTf] to the amido complex (IPr)Cu(NHPh), the calculated $\Delta\delta$ is 42.4 ppm. In contrast, for the W(II) d^4 complexes, the conversion of W-NH$_2$Ph to W-NHPh results in an experimentally determined *upfield* chemical shift with $\Delta\delta = -55.8$ ppm.

Although multiple factors could potentially contribute to the reversal in $\Delta\delta$ for the Ru, Pt and Cu complexes in comparison to the W systems, the most conspicuous culprit is the impact of d electron count, which could substantially influence the ΔE^{-1} term in the σ_p parameter (Eq (1)). In this equation, ΔE is the electronic excitation energy, which can be approximated by the HOMO–LUMO gap (*i.e.* the lowest energy electronic transition) [73]. Ignoring other factors that contribute to the paramagnetic screening term, as ΔE is decreased a downfield chemical shift is anticipated in the ^{15}N NMR spectrum and vice versa. Note from Table 3 that the W–amine complex has the smallest calculated HOMO–LUMO gap.

As previously described by Templeton *et al.* [16], for [Tp*W(CO)(PhC≡CMe)(NH$_n$Ph)]$^{m+}$ ($n = 1$, $m = 0$; $n = 2$, $m = 1$), in the absence of W–N π interactions, it is anticipated that the dπ orbitals will split into: (1) a lowest energy molecular orbital that has d$_{yz}$ character and results from back-bonding with the CO and alkyne

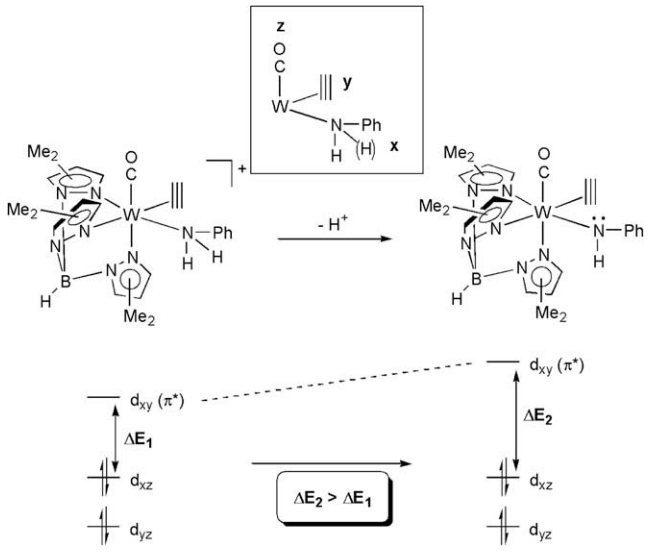

Scheme 2. Depiction of qualitative molecular orbital diagram for [Tp*W(CO)(PhC≡CMe)(NH$_2$Ph)]$^+$ and Tp*W(CO)(PhC≡CMe)(NHPh) illustrating anticipated impact on HOMO–LUMO gap upon conversion of the aniline complex to the amido complex.

ligands, (2) a middle energy π molecular orbital that is comprised of d_{xz}, which back-bonds with CO only, and (3) a highest energy orbital that has d_{xy} character, which is a π^* molecular orbital that results from alkyne-to-tungsten π-donation (Scheme 2). When comparing the amine and amido complexes, the lone pair on the amido orients to π-donate into d_{xy}, which results in an increase in the energy of this molecular orbital relative to that of the amine complex (Scheme 2). The net result is an increase in the HOMO–LUMO gap upon conversion of W–amine to W–amido, and if this term dominates σ_p an upfield chemical shift is anticipated for the amido complex relative to the amine complex.

For systems in which amido-to-metal π-donation is disrupted by a filled dπ manifold a different scenario unfolds. With a filled d orbital set, the lowest energy electronic excitation is anticipated to result from the transition of an electron in a metal-based orbital with metal-amido π anti-bonding character to either a ligand based anti-bonding orbital or a metal-ligand σ^* molecular orbital (Scheme 3). Protonation of the amido removes metal–N π-bonding and, hence, removes the anti-bonding character from the metal-based HOMO. Although this evaluation does not take into account the impact of protonation on other orbitals, it could be anticipated that the lowest energy electronic excitation might be decreased upon conversion of amine to amido as shown in Scheme 3, which is opposite of the prediction for the W(II) complex.

UV–Visible data for the lowest energy electronic transition for the series of complexes studied herein follow the predicted trends in Schemes 2 and 3 (Table 4). The Ru(II), Pt(IV) and Cu(I) complexes are all colorless in pure form, which is consistent with the absence of electronic transitions in the visible region for these systems. In contrast, the colored W(II) complexes exhibit absorptions above 500 nm. For the W(II) complexes, the cationic amine complex $[Tp^*W(CO)(PhC{\equiv}CMe)(NH_2Ph)]^+$ displays an absorption at 582 nm, while the amido complex $Tp^*W(CO)(PhC{\equiv}CMe)(NHPh)$ has an absorption at 543 nm. In contrast to this significant blue shift, for the Ru(II), Cu(I) and Pt(IV) systems amine to amido

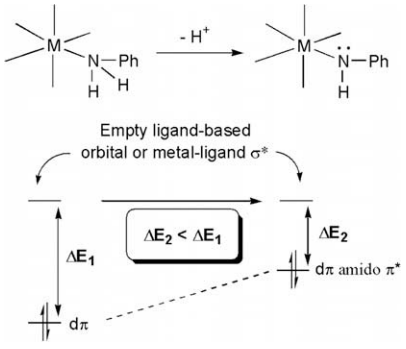

Scheme 3. Depiction of qualitative molecular orbital diagram for amine and amido complexes for metals with filled dπ manifold.

Table 4
Lowest energy absorption taken from UV–vis spectra.

Complex	λ (nm)	Δλ[a] (nm)
$TpRu(PMe_3)_2(NHPh)$	360	93
$[TpRu(PMe_3)_2(NH_2Ph)][OTf]$	267	
$(NCN)Pt(Me)_2NHPh$	319	23
$[(NCN)Pt(Me)_2(NH_2Ph)][BAr'_4]$	296	
(IPr)Cu(NHPh)	366	81
$[(IPr)Cu(NH_2Ph)][OTf]$	285	
$Tp^*W(CO)(\eta^2\text{-}PhC{\equiv}CMe)(NHPh)$	543	−39
$[Tp^*W(CO)(\eta^2\text{-}PhC{\equiv}CMe)(NH_2Ph)][BAr'_4]$	582	

[a] $\lambda_{amido} - \lambda_{amine}$.

conversions all result in a decrease in energy (red shift) for the lowest energy electronic excitation.

The QSPR analysis indicated a weak connection between HOMO–LUMO gap and ^{15}N NMR chemical shift. However, comparison of UV–Vis data and ^{15}N NMR chemical shifts for the W(II) amine and amido complexes versus the Ru(II) and Pt(IV) complexes suggests that amido-to-metal π-bonding plays an important role. These results seemingly contrast one another; however, due to the enormous difference in calculated and experimental chemical shift for the W(II) amido complex, this system was removed from the QSPR analysis. Hence, the QSPR analysis is based on d^6 and d^{10} metals for which amido-to-metal π-interaction is negligible, and the analysis likely provides an accurate reflection of the lack of impact for those systems. For the W(II) amine and amido complexes, amido-to-W π-bonding may dramatically alter the chemical shift for the amido complex.

3. Conclusions

^{15}N NMR chemical shifts have been collected for a series of transition metal amido and amine complexes. The combined experimental and computational data suggest that amido-metal π-interaction plays an important role in the change in chemical shift upon conversion of amine to amido. In the absence of amido-metal π-bonding, which results from filled d orbitals, *downfield* chemical shifts of 40–60 ppm are observed. However, for the W(II) complexes, the conversion of amine to amido results in an *upfield* chemical shift of almost 56 ppm, which is likely attributable to amido-to-tungsten π-donation. Thus, the difference in presence/absence of amido-to-metal π-bonding alters the chemical shift change by approximately 100 ppm.

4. Experimental

4.1. Materials

All solvents were degassed by N_2 (g) purging prior to use. Tetrahydrofuran-d_8 was used from freshly opened ampules purchased from Cambridge Isotope Laboratories, Inc. Tetrahydrofuran was purified by distillation from sodium/benzophenone. (IPr)Cu(NHPh) [61], $[(IPr)Cu(NH_2Ph)][OTf]$ [34], $(NCN)PtMe_2(NHPh)$ [63], $[(NCN)PtMe_2(NH_2Ph)][BAr'_4]$ [63], $TpRu(PMe_3)_2(NHPh)$ [62], $[TpRu(PMe_3)_2(NH_2Ph)][OTf]$ [62], $Tp^*W(CO)(PhC{\equiv}CMe)(NHPh)$ [16] and $[Tp^*W(CO)(PhC{\equiv}CMe)(NH_2Ph)][BAr'_4]$ [16] were prepared according to published procedures. The ^{15}N labeled complexes, $TpRu(PMe_3)_2(^{15}NHPh)$ and $[TpRu(PMe_3)_2(^{15}NH_2Ph)][OTf]$, have been previously reported including $^1J_{NH}$ data [82].

4.2. Measurements

All reactions and procedures were performed under anaerobic conditions in a nitrogen filled glovebox or using standard Schlenk techniques. Glovebox purity was maintained by periodic nitrogen purges and monitored by an oxygen analyzer {O_2(g) < 15 ppm for all reactions}. Single bond (^1H, ^{15}N) chemical shift correlation spectra were recorded on a Varian Mercury 400 MHz spectrometer operating at 40 MHz in the inverse mode using ^1H detection based on the HSQC method with ^{15}N decoupling using GARP (Globally Optimized Alternating Phase Rectangular Pulse). Two sets of 256 time increments were obtained in the phase-sensitive mode, processed to a final size of 2 K × 2 K; 64 transients were obtained per time increment and the relaxation delay was 1 s. Standard 1D ^{15}N NMR spectra were recorded from ^{15}N isotopically enriched samples via ^1H decoupled experiments operating at 40 MHz. All NMR samples were made from nearly saturated solutions of the

analyte in tetrahydrofuran-d_8. UV–Vis data was obtained via a Varian Cary 100 Bio UV–Vis spectrophotometer operated by the Varian Cary WinUV program was used to acquire UV–Vis data. Samples were acquired in THF solutions in screw cap quartz cells with path length of 1 cm. A blank spectrum of THF was subtracted from the sample spectra to observe the analyte.

4.3. Computational methods

Calculations employed the GAUSSIAN 03 suite of programs [83]. After calibration of a variety of computational techniques versus experimental data for aniline and LiNHPh, the following scheme was found to provide the best balance between computational efficiency and accuracy. All complexes were first optimized using B3LYP/CEP-31G(d) methods, the latter designating the Steven effective core potentials [84] for all heavy atoms with main group basis sets augmented by a d polarization function (taken from the 6-31G(d) basis set). The minima thus obtained were then submitted to a single point calculation of NMR properties using the Steven's CEP-31G basis set for the transition metal, 6-31G(d) for main group elements and the IGLO-III basis set [85,86] for the nitrogen atom whose NMR chemical shift was of interest. The BHandHLyp density functional was used for the calculation of the NMR chemical shifts as this was found to give the most reliable results on the basis of test calculations for $PhNH_2$ and LiNHPh. The NMR shifts were calculated using the GIAO approximation [87] in both the gas-phase and in solution (CPCM solvent model [88], Pauling radii, THF solvent). Calculated ^{15}N NMR chemical shifts are referenced to the value calculated for aniline at the same level of theory. In general, starting geometries for DFT optimizations were obtained from the lowest energy conformations obtained from a molecular mechanics based conformational search (metal and ligating atoms frozen) using the MOE software and the MMFF94x force field. When appropriate, different coordination isomers (cis/trans, fac/mer, *etc.*) were manually constructed and evaluated to obtain the lowest energy geometries used for subsequent NMR calculations.

Acknowledgements

The National Science Foundation (CAREER Award; CHE 0238167) is acknowledged by TBG for support of this research. TRC acknowledges the partial support of this research from the National Science Foundation through grant CHE-0701247. TRC also acknowledges the Chemical Computing Group for generously providing the MOE software and the NSF-CRIF program (CHE-0741936) for their support of the computational facilities used for the calculations. The authors also wish to thank Dr. Sabapathy Sankar (North Carolina State University) for his assistance in obtaining the ^{15}N NMR spectra, Prof. Elon Ison (North Carolina State University) for use of his UV–Vis spectrometer, and Prof. Jochen Autschbach (SUNY-Buffalo) for advice on NMR calculations.

Appendix A. Supplementary material

Supplementary data associated with this article can be found, in the online version, at doi:10.1016/j.jorganchem.2009.01.006.

References

[1] R. Kempe, Angew. Chem., Int. Ed. 39 (2000) 468–493.
[2] T.B. Gunnoe, Eur. J. Inorg. Chem. (2007) 1185–1203.
[3] H.E. Bryndza, W. Tam, Chem. Rev. 88 (1988) 1163–1188.
[4] J.R. Fulton, A.W. Holland, D.J. Fox, R.G. Bergman, Acc. Chem. Res. 35 (2002) 44–56.
[5] P.L. Holland, R.A. Andersen, R.G. Bergman, Comments Inorg. Chem. 21 (1999) 115–129.
[6] M.D. Fryzuk, C.D. Montgomery, Coord. Chem. Rev. 95 (1989) 1–40.
[7] A.R. Muci, S.L. Buchwald, Top. Curr. Chem. 219 (2002) 131–209.
[8] J.F. Hartwig, Pure Appl. Chem. 76 (2004) 507–516.
[9] R.R. Schrock, A.H. Hoveyda, Angew. Chem., Int. Ed. 42 (2003) 4592–4633.
[10] K.L. Breno, M.D. Pluth, D.R. Tyler, Organometallics 22 (2003) 1203–1211.
[11] D.E. Wigley, Prog. Inorg. Chem. 42 (1994) 239–482.
[12] R.A. Eikey, M.M. Abu-Omar, Coord. Chem. Rev. 243 (2003) 83–124.
[13] P. Müller, C. Fruit, Chem. Rev. 103 (2003) 2905–2919.
[14] L. Luan, P.S. White, M. Brookhart, J.L. Templeton, J. Am. Chem. Soc. 112 (1990) 8190–8192.
[15] K.R. Powell, P.J. Pérez, L. Luan, S.G. Feng, P.S. White, M. Brookhart, J.L. Templeton, Organometallics 13 (1994) 1851–1864.
[16] L.W. Francisco, P.S. White, J.L. Templeton, Organometallics 16 (1997) 2547–2555.
[17] B.K. Bennett, T.J. Crevier, D.D. DuMez, Y. Matano, W.S. McNeil, J.M. Mayer, J. Organomet. Chem. 591 (1999) 96–103.
[18] J.D. Soper, B.K. Bennett, S. Lovell, J.M. Mayer, Inorg. Chem. 40 (2001) 1888–1893.
[19] J.D. Soper, W. Kaminsky, J.M. Mayer, J. Am. Chem. Soc. 123 (2001) 5594–5595.
[20] M.D. Curtis, J. Real, J. Am. Chem. Soc. 108 (1986) 4668–4669.
[21] W.E. Buhro, M.H. Chisholm, K. Folting, J.C. Huffman, J. Am. Chem. Soc. 109 (1987) 905–906.
[22] P.J. Pérez, L. Luan, P.S. White, M. Brookhart, J.L. Templeton, J. Am. Chem. Soc. 114 (1992) 7928–7929.
[23] J.Y.K. Tsang, C. Fujita-Takayama, M.S.A. Buschhaus, B.O. Patrick, P. Legzdins, J. Am. Chem. Soc. 128 (2006) 14762–14763.
[24] S.G. Feng, P.S. White, J.L. Templeton, Organometallics 14 (1995) 5184–5192.
[25] D.M. Giolando, K. Kirschbaum, L.J. Graves, U. Bolle, Inorg. Chem. 31 (1992) 3887–3890.
[26] H.J. Banbery, F. Mcquillan, T.A. Hamor, C.J. Jones, J.A. Mccleverty, Polyhedron 8 (1989) 559–561.
[27] K.G. Caulton, New J. Chem. 18 (1994) 25–41.
[28] J.M. Mayer, Comments Inorg. Chem. 8 (1988) 125–135.
[29] J.R. Fulton, M.W. Bouwkamp, R.G. Bergman, J. Am. Chem. Soc. 122 (2000) 8799–8800.
[30] K.N. Jayaprakash, D. Conner, T.B. Gunnoe, Organometallics 20 (2001) 5254–5256.
[31] E.D. Blue, A. Davis, D. Conner, T.B. Gunnoe, P.D. Boyle, P.S. White, J. Am. Chem. Soc. 125 (2003) 9435–9441.
[32] D. Conner, K.N. Jayaprakash, T.R. Cundari, T.B. Gunnoe, Organometallics 23 (2004) 2724–2733.
[33] D. Conner, K.N. Jayaprakash, M.B. Wells, S. Manzer, T.B. Gunnoe, P.D. Boyle, Inorg. Chem. 42 (2003) 4759–4772.
[34] C. Munro-Leighton, E.D. Blue, T.B. Gunnoe, J. Am. Chem. Soc. 128 (2006) 1446–1447.
[35] C. Munro-Leighton, S.A. Delp, N.M. Alsop, E.D. Blue, T.B. Gunnoe, Chem. Commun. (2008) 111–113.
[36] C. Munro-Leighton, S.A. Delp, E.D. Blue, T.B. Gunnoe, Organometallics 26 (2007) 1483–1493.
[37] L.A. Goj, E.D. Blue, S.A. Delp, T.B. Gunnoe, T.R. Cundari, A.W. Pierpont, J.L. Petersen, P.D. Boyle, Inorg. Chem. 45 (2006) 9032–9045.
[38] J.R. Fulton, S. Sklenak, M.W. Bouwkamp, R.G. Bergman, J. Am. Chem. Soc. 124 (2002) 4722–4737.
[39] Y. Feng, M. Lail, K.A. Barakat, T.R. Cundari, T.B. Gunnoe, J.L. Petersen, J. Am. Chem. Soc. 127 (2005) 14174–14175.
[40] Y. Feng, T.B. Gunnoe, T.V. Grimes, T.R. Cundari, Organometallics 25 (2006) 5456–5465.
[41] J. Zhang, T.B. Gunnoe, P.D. Boyle, Organometallics 23 (2004) 3094–3097.
[42] J. Zhang, T.B. Gunnoe, J.L. Petersen, Inorg. Chem. 44 (2005) 2895–2907.
[43] K.N. Jayaprakash, T.B. Gunnoe, P.D. Boyle, Inorg. Chem. 40 (2001) 6481–6486.
[44] D.J. Fox, R.G. Bergman, J. Am. Chem. Soc. 125 (2003) 8984–8985.
[45] D.J. Fox, R.G. Bergman, Organometallics 23 (2004) 1656–1670.
[46] T.K.G. Erikson, J.C. Bryan, J.M. Mayer, Organometallics 7 (1988) 1930–1938.
[47] J.M. Mayer, C.J. Curtis, J.E. Bercaw, J. Am. Chem. Soc. 105 (1983) 2651–2660.
[48] S.E. Kegley, C.J. Schaverien, J.H. Freudenberger, R.G. Bergman, J. Am. Chem. Soc. 109 (1987) 6563–6565.
[49] D.S. Glueck, R.G. Bergman, Organometallics 10 (1991) 1479–1486.
[50] D.S. Glueck, L.J.N. Winslow, R.G. Bergman, Organometallics 10 (1991) 1462–1479.
[51] D.S. Glueck, J. Wu, F.J. Hollander, R.G. Bergman, J. Am. Chem. Soc. 113 (1991) 2041–2054.
[52] J.F. Hartwig, R.G. Bergman, R.A. Andersen, J. Am. Chem. Soc. 113 (1991) 6499–6508.
[53] P.L. Holland, R.A. Andersen, R.G. Bergman, J. Huang, S.P. Nolan, J. Am. Chem. Soc. 119 (1997) 12800–12814.
[54] A.W. Holland, R.G. Bergman, J. Am. Chem. Soc. 124 (2002) 14684–14695.
[55] G.L. Hillhouse, J.E. Bercaw, J. Am. Chem. Soc. 106 (1984) 5472–5478.
[56] H.E. Bryndza, L.K. Fong, R.A. Paciello, W. Tam, J.E. Bercaw, J. Am. Chem. Soc. 109 (1987) 1444–1456.
[57] D.J. Mindiola, G.L. Hillhouse, J. Am. Chem. Soc. 123 (2001) 4623–4624.
[58] Y.M. Badiei, A. Krishnaswamy, M.M. Melzer, T.H. Warren, J. Am. Chem. Soc. 128 (2006) 15056–15057.
[59] P.R. Sharp, J. Chem. Soc., Dalton Trans. (2000) 2647–2657.
[60] S.A. Delp, C. Munro-Leighton, L.A. Goj, M.A. Ramirez, T.B. Gunnoe, J.L. Petersen, P.D. Boyle, Inorg. Chem. 46 (2007) 2365–2367.

[61] L.A. Goj, E.D. Blue, C. Munro-Leighton, T.B. Gunnoe, J.L. Petersen, Inorg. Chem. 44 (2005) 8647–8649.
[62] D. Conner, K.N. Jayaprakash, T.B. Gunnoe, P.D. Boyle, Inorg. Chem. 41 (2002) 3042–3049.
[63] C. Munro-Leighton, Y. Feng, J. Zhang, N.M. Alsop, T.B. Gunnoe, P.D. Boyle, J.L. Petersen, Inorg. Chem. 47 (2008) 6124–6126.
[64] I.M. Lagoja, P. Herdewijn, Synthesis (2002) 301–314.
[65] A. Laxer, D.T. Major, H.E. Gottlieb, B. Fischer, J. Org. Chem. 66 (2001) 5463–5481.
[66] C. Kojima, A.M. Ono, A. Ono, M. Kainosho, Methods Enzymol. 338 (2001) 261–283.
[67] B. Schneider, Planta 203 (1997) 1–8.
[68] M. Andreis, J.L. Koenig, Application of nitrogen-15 NMR to polymers, Polysoaps/Stabilizers/Nitrogen-15 Nmr, 1995, pp. 191–237.
[69] G.V. Fazakerley, Y. Boulard, Methods Enzymol. 261 (1995) 145–163.
[70] R.K. Harris, M.J. Leach, D.P. Thompson, Chem. Mater. 4 (1992) 260–267.
[71] E.L. Sceats, J.S. Figueroa, C.C. Cummins, N.M. Loening, P. Van, R. der Wel, G. Griffin, Polyhedron 23 (2004) 2751–2768.
[72] Y. Tanaka, A. Ono, Dalton Trans. (2008) 4965–4974.
[73] J. Mason, Chem. Rev. 81 (1981) 205–227.
[74] J. Mason, L.F. Larkworthy, E.A. Moore, Chem. Rev. 102 (2002) 913–934.
[75] L. Carlton, R. Weber, Magn. Reson. Chem. 35 (1997) 817–820.
[76] J. Mason, Encyclopedia of Nuclear Magnetic Resonance, Wiley, New York, 1996.
[77] S. Ide, K. Iwasawa, A. Yoshino, T. Yoshida, K. Takahashi, Mag. Res. Chem. 25 (1987) 675–679.
[78] J.B. Lambert, G. Binsch, J.D. Roberts, Proc. N. A. S. 51 (1964) 735–737.
[79] D.B. Grotjahn, P.M. Sheridan, I. Al Jihad, L.M. Ziurys, J. Am. Chem. Soc. 123 (2001) 5489–5494.
[80] G.C. Levy, R.L. Lichter, Nitrogen-15 Nuclear Magnetic Resonance Spectroscopy, Wiley, New York, 1979.
[81] MOE Program; Chemical Computing Group, Version 2005, 2006. <http://www.chemcomp.com/>.
[82] Y.E. Feng, M. Lail, N.A. Foley, T.B. Gunnoe, K.A. Barakat, T.R. Cundari, J.L. Petersen, J. Am. Chem. Soc. 128 (2006) 7982–7994.
[83] GAUSSIAN 03, Revision D.01, M.J. Frisch, G.W. Trucks, H.B. Schlegel, G.E. Scuseria, M.A. Robb, J.R. Cheeseman, J.A. Montgomery Jr., T. Vreven, K.N. Kudin, J.C. Burant, J.M. Millam, S.S. Iyengar, J. Tomasi, V. Barone, B. Mennucci, M. Cossi, G. Scalmani, N. Rega, G.A. Petersson, H. Nakatsuji, M. Hada, M. Ehara, K. Toyota, R. Fukuda, J. Hasegawa, M. Ishida, T. Nakajima, Y. Honda, O. Kitao, H. Nakai, M. Klene, X. Li, J.E. Knox, H.P. Hratchian, J.B. Cross, V. Bakken, C. Adamo, J. Jaramillo, R. Gomperts, R.E. Stratmann, O. Yazyev, A.J. Austin, R. Cammi, C. Pomelli, J.W. Ochterski, P.Y. Ayala, K. Morokuma, G.A Voth, P. Salvador, J.J. Dannenberg, V.G. Zakrzewski, S. Dapprich, A.D. Daniels, M.C. Strain, O. Farkas, D.K. Malick, A.D. Rabuck, K. Raghavachari, J.B. Foresman, J.V. Ortiz, Q. Cui, A.G. Baboul, S. Clifford, J. Cioslowski, B.B. Stefanov, G. Liu, A. Liashenko, P. Piskorz, I. Komaromi, R.L. Martin, D.J. Fox, T. Keith, M.A. Al-Laham, C.Y. Peng, A. Nanayakkara, M. Challacombe, P.M.W. Gill, B. Johnson, W. Chen, M.W. Wong, C. Gonzalez, J. A. Pople, Gaussian, Inc., Wallingford, CT, 2004.
[84] W.J. Stevens, M. Krauss, H. Basch, P.G. Jasien, Can. J. Chem. 70 (1992) 612–630.
[85] W. Kutzelnigg, U. Fleischer, M. Schindler, in: P. Diehl, E. Fluck, E. Kosfeld (Eds.), NMR: Basic Principles and Progress, Springer, Berlin, 1991, pp. 165–262.
[86] For a recent application of these basis sets see C. Scheurer, N.R. Skrynnikov, S.F. Lienin, S.K. Straus, R. Bruschweiler, R.R. Ernst, J. Am. Chem. Soc. 121 (1999) 4242–4251.
[87] J. Gauss, J.F. Stanton, Adv. Chem. Phys. 123 (2002) 355–422.
[88] J. Tomasi, B. Mennucci, R. Cammi, Chem. Rev. 105 (2005) 2999–3093.